Disinfection during Iron Electrocoagulation

Differentiating between Inactivation and Floc Entrapment for Escherichia coli and Somatic Coliphage Øx174

Bicudo, Bruno; Van Der Werff, Bart Jan; Medema, Gertjan; Van Halem, Doris

DOI
10.1021/acsestwater.2c00230

Publication date
2022

Document Version
Final published version

Published in
ACS ES and T Water

Citation (APA)
Bicudo, B., Van Der Werff, B. J., Medema, G., & Van Halem, D. (2022). Disinfection during Iron Electrocoagulation: Differentiating between Inactivation and Floc Entrapment for Escherichia coli and Somatic Coliphage Øx174. *ACS ES and T Water*, *2*(10), 1707-1714. https://doi.org/10.1021/acsestwater.2c00230

ACS ES&T Water

pubs.acs.org/estwater

Article

Disinfection during Iron Electrocoagulation: Differentiating between Inactivation and Floc Entrapment for *Escherichia coli* and Somatic Coliphage ØX174

Bruno Bicudo,* Bart-Jan van der Werff, Gertjan Medema, and Doris van Halem

Cite This: https://doi.org/10.1021/acsestwater.2c00230

Read Online

ACCESS | Metrics & More | Article Recommendations

ABSTRACT: Electrochemical water treatment is gaining increasing popularity due to its wide range of potential applications, its decreasing costs, and its suitability as a decentralized treatment alternative, but mainly due to it being considered a "green technology". In the field of municipal wastewater treatment, the use of iron electrocoagulation (Fe-EC) has been marginal and although disinfection has been reported, its underlying mechanisms are not fully understood, for which significant controversy remains. In this study, microbial inactivation during Fe-EC was evaluated as a two-component process, namely, physical removal by microbial floc sorption/entrapment, and inactivation by reactive oxygen species (ROS) produced by (semi)Fenton reactions. Using the fecal indicators *Escherichia coli* WR1 and somatic coliphage ØX174 suspended in a synthetic water matrix, the role of ROS and the role of flocculation were quantitatively evaluated. Fenton inhibitor TEMPOL was used to quench ROS production during Fe-EC. At circumneutral pH, ROS were found to be highly detrimental to *E. coli*, yet only mildly damaging for phage ØX174 (≈3.9 $\log_{10}$ and ≈0.8 $\log_{10}$ inactivation, respectively). Inactivation for both indicators increased under acidic conditions (pH 5.5), likely due to the formation of hydroxyl radicals ($^{\bullet}OH$), exceeding 5.1 $\log_{10}$ for *E. coli* and 1.5 $\log_{10}$ for phage ØX174. The ROS inactivation pathway is linked to the oxidation of ferrous iron (Fe^{2+}), being independent of flocculation settings. Experiments involving different flocculation settings demonstrated that there is a strong positive correlation between orthokinetic-like flocculation conditions, floc sedimentation, and microbial removal, meaning that floc entrapment is a major removal pathway following Fe-EC. When compared to control experiments in which no proper flocculation stage was introduced, orthokinetic flocculation produced additional 3.1 $\log_{10}$ and 4.4 $\log_{10}$ removal for *E. coli* and phage ØX174, respectively. We conclude that ROS production is not a prerequisite for removal of *E. coli* and phage ØX174, however, it does offer an additional disinfection barrier, which increases the robustness of Fe-EC for water treatment.

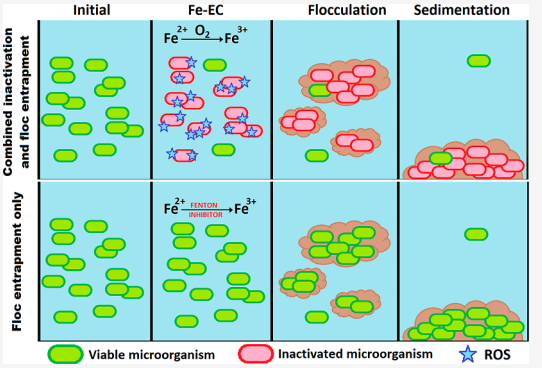

KEYWORDS: *iron electrocoagulation, disinfection, reactive oxygen species, orthokinetic flocculation, water treatment*

1. INTRODUCTION

Water reclamation is a generic name for processes designed to turn municipal sewage or industrial effluents into water that can be used for a wide range of purposes, from drinking, irrigation, aquaculture, dust control, and cooling to cleaning or construction.[1,2] According to FAO,[3] the largest consumer of reclaimed water globally is agriculture, accounting for over 20 million hectares irrigated in over 50 countries, 10% of the world's croplands. Despite the obvious advantages of wastewater reclamation, such as reducing pressure on freshwater sources and avoiding pollution in receiving waterbodies, it still carries important health risks to its users, as reclaimed water may harbor a wide range of pathogenic microorganisms. These include helminth eggs, bacteria, viruses, and protozoa that are associated with a high disease burden now, and (emerging) antibiotic-resistant bacteria, regarded as one of the most significant threats to global health by the WHO.[4] As a result, municipal effluent reclamation demands special attention for its associated health risks, which will vary according to the type of water reuse, susceptibility and exposure routes of its users, and concentration of pathogens in the reclaimed effluents. Therefore, the extent to which sewage requires to be treated for adequate reuse is both a function of the specific reuse intended and the probability of its users being exposed to it.

In this research, we explore the microbial disinfection[a] mechanisms produced during iron electrocoagulation (Fe-EC)

Received: May 20, 2022
Revised: August 20, 2022
Accepted: August 22, 2022

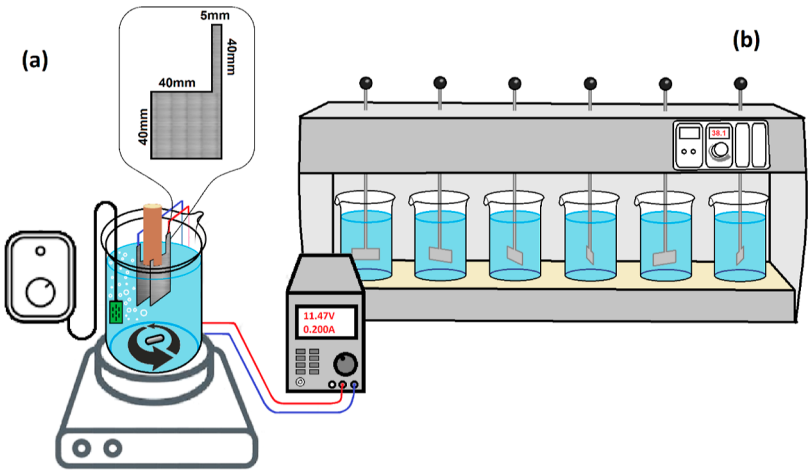

Figure 1. Experimental setup; (a) Fe-EC unit with DC magnetic mixing, power supply, air supply, details of size and shape of Fe electrodes, and (b) jar test used for flocculation/sedimentation.

for water reclamation, as previous studies have highlighted its benefits for organic micropollutant (OMP) degradation as well as nutrients, heavy metals, and arsenic removal.[5−10] During Fe-EC, an electric current is conducted between two (or more) electrodes immersed in a liquid. As a consequence, metallic Fe^0 constituting the anode will dissolve as Fe^{2+} into the solution,[11−13] while on the surface of the cathode water molecules are reduced to OH^- and H_2, as indicated in eqs 1 and 2.

$$Fe^0 \rightarrow Fe^{2+} + 2e^- \quad (1)$$

$$2H_2O + 2e^- \rightarrow 2OH^- + H_2 \quad (2)$$

The overall reaction facilitated by Fe-EC is then as follows 3

$$Fe^0 + 2H_2O \rightarrow Fe^{2+}\,2OH^- + H_2(g) \quad (3)$$

In the presence of dissolved oxygen (DO), the reaction described by eq 3 further progresses and insoluble hydroxides are formed, typically in the form of amorphous $Fe(OH)_3$, as displayed in eq 4

$$4Fe^{2+} + 10H_2O + O_2 \rightarrow 4Fe(OH)_3 + 8H^+ \quad (4)$$

Fe-EC is especially advantageous in off-grid applications in which coagulant supply chains and storage are difficult. It also offers notable advantages over traditional Fe-salt coagulation: the H_2 production in the cathode aids in floc removal by flotation, it does not react with alkalinity and it does not increase conductivity because the Fe is directly dissolved into the solution without the need of a counter ion in the salt. However, the dosage of chemical coagulants can be performed regardless of the water conductivity and instantaneously in a single injection, while EC requires current and time (as described by Faraday's law) and a sufficiently conductive liquid. If the process is conducted under aerobic conditions, then Fe^{2+} will further oxidize to Fe^{3+}. It is during the ferrous Fe oxidation process that a series of so-called reactive oxygen species (ROS) are produced, some of which have been identified as powerful oxidizing agents with attractive disinfectant properties. This ROS pathway starts with the production of the superoxide radical ($^{\bullet}O_2^-$), which progresses into H_2O_2 to trigger a Fenton process, finishing with either a hydroxyl radical ($^{\bullet}OH$) or highly valent Fe species such as ferryl radical (Fe(IV)) depending on the pH.[14] Under acidic conditions (pH < 6), the predominant species will be the hydroxyl radical, while under more basic conditions ferryl radical will predominate.[14,38] Inactivation by ROS is a consequence of severe oxidative damage to proteins, enzymes, deoxyribonucleic, and ribonucleic acids (DNA/RNA), viral capsids and phospholipid envelopes, damage and rupture of cellular membranes, or the interruption of the cellular respiratory pathways,[15−18] and disinfection by ROS has been reported by several researchers.[7,22,25,30,38] The hydroxyl and ferryl radicals are the most detrimental to microbial cells, as these lack enzymatic deactivation pathways against them.[19,20] ROS-mediated inactivation by oxidizing Fe^{2+} has received increasing attention, particularly for virus and bacterial inactivation,[17,21−25] although the inactivation kinetics associated with it are still not fully understood. To make the issue more complex, ROS inactivation is not the only process associated with microbial disinfection during Fe-EC, as microorganisms are to a very large extent trapped and/or adsorbed into the hydrolysis products, typically insoluble Fe(III)-hydroxides. These two processes are not only just simultaneous but also coincide spatially and target the same microorganisms, rendering the characterization of each disinfection process conceptually challenging. The objective of this research was therefore to differentiate between Fe-EC disinfection pathways, specifically ROS-induced inactivation versus floc entrapment.

To do so, Fe-EC experiments were conducted at various pH, flocculation conditions, and under the presence/absence of an ROS quencher using water containing the bacterium *E. coli* and somatic coliphage virus ØX174, given their extensive use as fecal indicators in the water research field.[26,27]

2. MATERIALS AND METHODS

2.1. Water Matrix and Microbial Indicators. Experiments were conducted using a water matrix comprised demineralized water, and 175 mg/L NaCl was added for conductivity purposes as well as to create an osmotic pressure similar to that of the spiked microbial indicators. Non-pathogenic microbial indicators were selected to be spiked into the test water, namely, *E. coli* WR1 (NCTC 13167) and somatic coliphage ØX174 (ATCC 13706-B1). Dilution buffer for all experiments was phosphate-buffered saline (PBS), with a buffer strength of 0.01 M phosphate buffer and a pH of 7.3 ±

https://doi.org/10.1021/acsestwater.2c00230
ACS EST Water XXXX, XXX, XXX−XXX

0.1. Propagation of *E. coli* WR1 was performed in a tryptone yeast extract glucose broth (TYGB) incubated at 37 °C to concentrations of ≈1 × 10^8 cfu/mL, centrifuged, and re-suspended in PBS to concentrations of ≈1 × 10^9 cfu/mL, stored at 4 °C, and used within 24 h of production. Propagation of phage ØX174 was performed as per ISO 10705-2_2000,[44] obtaining concentrations ≈1 × 10^9 pfu/mL. For all experiments, the indicators were dosed at concentrations of ≈1 × 10^6 cfu/mL and 1 × 10^5 pfu/mL, respectively. Quantification of *E. coli* was performed by culture methods, either by membrane filtration or spread plating technique (depending on the expected concentration range) as described in APHA-standard methods for the examination of water and wastewater, 23rd Edition.[43] Chromocult Coliform Agar (Merck) was the selected medium for *E. coli* growth and quantification of colonies. Quantification of phage ØX174 was performed by pour-plate, as per ISO 10705-2_2000.

2.2. Laboratory Setup. Experiments were conducted in cylindrical 1 L glass beakers, as depicted in Figure 1. The power source was a dual 30 V−3 A TENMA 72-10500 bench DC supply, connected using crocodile clip cables to two parallel ARMCO steel plates (maximum percent-ages: 0.14% carbon, 0.10% silicium, 0.80% manganese, 0.025% phosphorous, 0.015% sulfur, 0.010% nitrogen, 0.20% copper, and 0.080% aluminum). The plates were square-shaped (40 × 40 mm) with a thin elongation protruding parallel to one of the sides (40 × 5 mm) in order for it to serve as a dry contact for the clip cables outside of the water. Before each use, plates were polished with coarse and fine sand paper and rinsed with demineralized water. Plates were then fitted in parallel slots carved at the end of a PVC tube, guaranteeing they remained parallel and spaced to exactly 10 mm from each other, as described elsewhere.[23,28−30] Beakers were fitted with magnetic PTFE-coated bars, placed on LABNICO L23 magnetic stirrers, and stirred during the course of the electric dosage. During all experiments, air was supplied continuously using an OASE OxyMax200 air pump to maintain oxygen saturation (>8 mgO_2/L). During the experiments, in which the effect of the flocculation/sedimentation was assessed, the beakers were moved into a Velp Scientifica JLT6 Jar test immediately after the application of the current had concluded. Settings for the jar test experiments are further described in Table 1.

Table 1. Flocculation and Sedimentation Settings

	flocculation	settling
Fe-EC only	no flocculation	no
no flocculation	no flocculation	4 h
poor flocculation	10 min@1000−1100 rpm with magnetic stirrer	
semiorthokinetic	10 min@100 rpm (G = 62 s^{-1}) with jar test	
full orthokinetic	10 min@100 rpm (G = 62 s^{-1}) + 10 min@50 rpm (G = 22 s^{-1}) with jar test	

2.3. Experimental Overview. For all experiments, Fe was dosed electrochemically by applying a constant 200 mA current during 15 min in 1 L beakers containing microbial suspensions, in order to produce a low current density (<20 mA/cm^2). With these settings, the theoretical Faradaic Fe dosage was of approximately 52.1 mgFe/L, according to Faraday's law of electrolysis.

Experiments, in which the effect of ROS in inactivation was assessed, were conducted under the presence or absence of the nitroxide 4-hydroxy-2,2,6,6-tetramethylpiperidin-1-oxyl (also known as 4-hydroxy-TEMPO or TEMPOL),[31] which was also performed under varying pH values. TEMPOL is a known Fenton inhibitor that promotes the catalysis of the superoxide radical, together with catalase-like destruction of H_2O_2, and the hindering of toxic hydroxyl radical production. It is the most studied nitroxide, due to its more affordable cost, high cell permeability, and low molecular weight.[32] Beakers selected for Fenton quenching were dosed with 200 mg of reagent grade TEMPOL (Sigma-Aldrich—Germany) in the crystal form, after weighing and dosing directly into the test beakers before the application of electric current. For the pH experiments, three levels of pH were selected, 5.5, 7.5, and 8.5. The stabilization of pH was conducted before the application of current by manually dosing HCl [1 M] or NaOH [1 M] and continued during the application of current. Three samples were produced during each experiment, namely, before the application of Fe-EC, immediately after the application of Fe-EC, and after 4 h of settling.

To examine the effect of flocculation on disinfection, five different flocculation settings were tested, ranging from no flocculation nor sedimentation, to proper orthokinetic flocculation with adequate settling time, immediately after the application of the electric charge. The characteristics of each mixing/settling condition (time, intensity, and mixing device) are described in Table 1.

The selected settings for the different mixing and sedimentation conditions were chosen to represent improving flocculation/sedimentation conditions, ranging from; (i) no sedimentation (Fe-EC only), (ii) Fe-EC and settling without flocculation (no flocculation), (iii) inadequate flocculation (poor flocculation), (iv) suboptimal flocculation (semi-orthokinetic), and (v) optimal flocculation (full orthokinetic). The latter represents standard orthokinetic flocculation conditions as recommended for municipal drinking water or chemical wastewater treatment throughout the design literature.[33−36] For experiments without flocculation or sedimentation, (Fe-EC only) bulk liquid samples were collected immediately after the current was removed, while for the rest of the assays, supernatant samples were collected after the 4 h sedimentation stage.

Samples of the mixed bulk liquid during and following Fe-EC were observed under a Keyence VHX digital microscope, in order to characterize the size and size distribution of the formed flocs. A large number of pictures (>25) was taken for each set of experiments, from which average floc area, and maximum/minimum floc diameter were obtained.

2.4. Statistical Analysis. Data series of somatic coliphage and *E. coli* inactivation were analyzed with the statistical test ANOVA (analysis of variance) in order to determine if the different pH conditions (Section 3.1) or flocculation conditions (Section 3.2) introduced statistically significant differences. In all cases, the obtained data were comprised triplicate microbial sampling in duplicate assays (n = 6). For microbial indicators presenting varying inactivation patterns under different settings, Tukey's (honest significance) range test was used to verify significance between all possible combinations of them.

2.5. Faraday's Law of Electrolysis. Faraday's law provides the numerical framework for the Fe-dosage calculations during the electrocoagulation process, as it allows to calculate the mass of Fe dissolved into the water matrix, as a

https://doi.org/10.1021/acsestwater.2c00230
ACS EST Water XXXX, XXX, XXX−XXX

function of the intensity of the current passed through it, and the electrolysis time (eq 5).

$$m = \frac{i \times t \times M}{n \times F} \quad (5)$$

where: m = mass of metal released into the solution (g), i = current intensity (A), t = time of current application (s), M = molar mass of the metal in question (for Fe = 55.84 g/mol), n = valence of the released metal ion (for Fe n = 2), and F = Faraday's constant (96,485.3 C mol^{-1}).

3. RESULTS

3.1. ROS-Induced Inactivation. To distinguish the contribution of ROS-inactivation produced during Fe-EC from physical separation produced during flocculation/sedimentation, the ROS quencher TEMPOL was added before the current was applied. For *E. coli*, results demonstrated that Fe-EC yielded 3.9 log_{10} removal in the bulk liquid, which dropped to 0.6 log_{10} in the presence of the ROS quencher. The ANOVA test confirmed that inactivation under quenched and non-quenched conditions is statistically different (p-value < 0.01). Hence, quenching of ROS prevented *E. coli* removal by 3.3 log_{10}. Phage ØX174 showed a very different behavior, as removal seemed to be unaffected by the presence of the ROS quencher (ANOVA p-value ≫ 0.05). During the Fe-EC process, ≈0.8 log_{10} removal was achieved for phage ØX174, which was significantly lower than for *E. coli* (Figure 2).

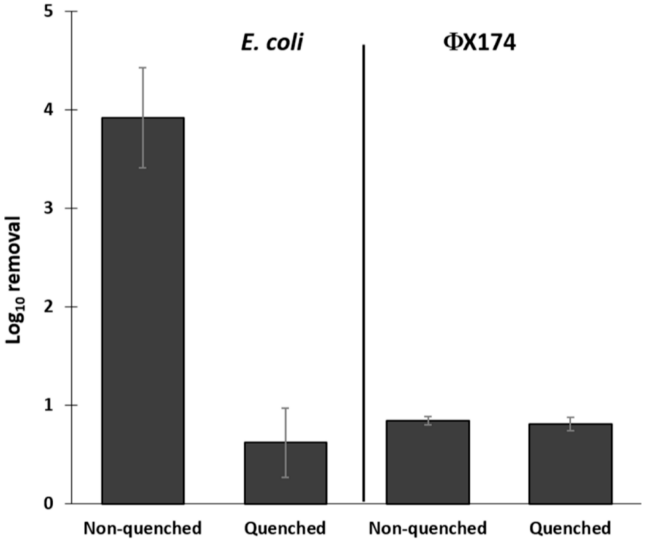

Figure 2. Log_{10} removal plot of *E. coli* WR1 and phage ØX174 immediately after Fe-EC (pH 7.5), in the absence (non-quenched) and presence (quenched) of the Fenton-inhibitor TEMPOL. Experiments were performed in duplicate, and microbial screening was performed in triplicate. Error bars indicate standard deviation.

The solution's pH has been reported to affect the ROS speciation, specifically for the Fenton reaction products $^{\bullet}OH$ (hydroxyl radical) and Ferryl Fe (FeIV), as the former is produced under acidic conditions (pH < 6), while the latter is predominant at more basic conditions (pH > 6).[14,37,38] The hydroxyl radical is regarded as a more potent inactivation agent than the high-valent Fe radical, implying that a fixed amount of oxidizing Fe^{2+} should be more detrimental to microorganisms if the oxidation is produced under more acidic conditions. In order to demonstrate this, similar quenching experiments were conducted using three different pH values, namely, pH 5.5 to achieve production of hydroxyl radical, pH 7.5 as in the previous experiments (similar to pH of secondary effluents), and a pH of 8.5 to promote production of high-valent Fe (FeIV). For all cases, the pH was kept constant during the Fe-EC by the addition of acid or base.

For *E. coli*, results indicate a better overall removal efficiency under acidic conditions (pH 5.5), exceeding 5.1 log_{10} (Figure 3). For pH 7.5 and 8.5, inactivation reduced to ≈3.9 log_{10} and

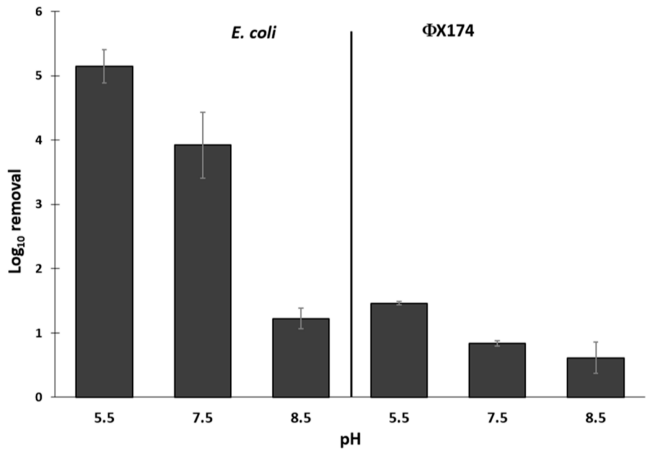

Figure 3. Log_{10} removal plot of *E. coli* WR1 and phage ØX174 after electrolysis under pH 5.5, 7.5, and 8.5. Experiments were performed in duplicate, and microbial screening was performed in triplicate. Error bars indicate standard deviation.

≈1.2 log_{10}, respectively. ANOVA and Tukey range tests point to a clear statistical difference between the three ROS inactivation plots (p-value < 0.01), indicating that ROS inactivation increases strongly with decreasing pH. This pH-dependent effect on *E. coli* inactivation is in-line with the reactivity of the produced Fenton intermediates, illustrating that the main driver in these experiments for *E. coli* attenuation was ROS-mediated inactivation. It is worth noting that for pH 5.5, even though 5.1 log_{10} inactivation was observed, Fe oxidation was incomplete to be 44−48% of Fe^{2+} still remained in solution. This means that in a scenario in which Fe^{2+} is fully oxidized into Fe^{3+}, *E. coli* ROS-inactivation is expected to be even higher, as larger amounts of ROS would be produced. This, however, was not achieved during the timespan of the experiments due to the low Fe^{2+} oxidation rate under acidic conditions.

For phage ØX174, results showed that the disinfection fraction attributable to ROS-mediated inactivation was significantly larger (≈1.5 log_{10}) for pH 5.5, than for pH 7.5 or 8.5. This could indicate a slightly larger sensitivity of phage ØX174 to the more aggressive hydroxyl radical, whose presence is expected at pH 5.5, but negligible at pH > 6. The ANOVA test identified a statistical difference between the ROS inactivation plots (p-value < 0.05), while the Tukey range test isolated such a difference between the pH 5.5 data set and the remaining two data sets (pH 7.5 and 8.5), indicating that ROS inactivation is statistically similar for pH 7.5 and 8.5, but increases significantly under acidic conditions.

3.2. Floc Entrapment. In order to unravel the contribution of removal by floc entrapment, experiments were conducted under different flocculation settings. The turbidity and residual Fe in the supernatant are presented in

https://doi.org/10.1021/acsestwater.2c00230
ACS EST Water XXXX, XXX, XXX−XXX

Table 2. Turbidity and Residual Fe Concentrations for the Five Assayed Flocculation Conditions

	Fe-EC only	No Flocculation	Poor Flocculation	Semi-orthokinetic	Full orthokinetic
			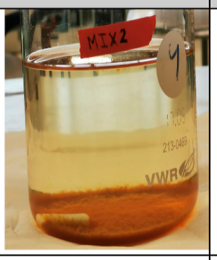		
Turbidity after Fe-EC (NTU)	69.7	66.3	67.9	70.4	70.1
Avg. turbidity after 4 h settling (NTU)	N/A	6.6	2.8	0.9	0.6
Avg. dosed total Fe (actual) (mg/L)	50.3	50.3	50.1	49.9	50.2
Supernatant total Fe after 4 h setling (mg/L)	N/A	4.80	1.80	0.25	0.11
Fe removal by settling (%)	N/A	90.4%	96.4%	99.5%	99.8%
E. coli removal (log_{10})	3.9	4.2	4.6	5.6	7.0
ØX174 removal (log_{10})	0.8	0.8	0.9	3.5	5.2

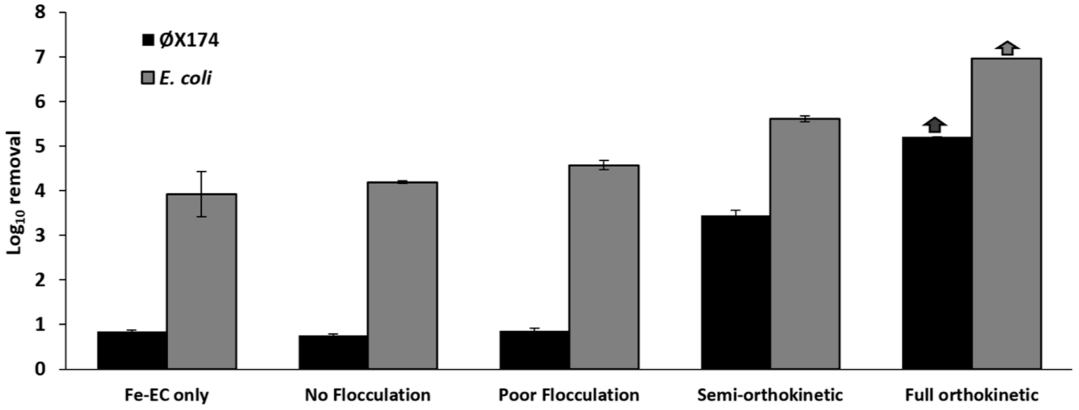

Figure 4. Log_{10} removal plot of phage ØX174 and *E. coli* for each flocculation configuration/removed Fe (%), following Fe-EC. Note: bars marked with an arrow (↑) indicate a minimum estimated removal due to microbial concentration below detection limit. Experiments were performed in duplicate, and microbial screening was performed in triplicate. Error bars indicate standard deviation.

Table 2, while details of the respective flocculation settings can be found in Table 1. Both turbidity and residual Fe in the supernatant decreased under improving flocculation conditions, average turbidity dropped from 68.9 NTU to 0.6 NTU, while residual Fe dropped from 50.2 to 0.11 mgFe/L. The Faradaic efficiency of the process was determined between 95.7 and 96.5%. It is worth noting that for all experiments, DO was maintained close to saturation (≥8.0 mgO_2/L) by pumping fine air bubbles into the beakers during the Fe-EC and that remaining Fe^{2+} was <0.1 mg/L for all samples.

The control experiment with Fe-EC only showed a concentration decrease of 3.9 log_{10} for *E. coli* and 0.8 log_{10} for phage ØX174, with all the dosed Fe still being in the suspension at the moment of sampling (Table 2). Subsequent experiments conducted under identical Fe-EC were subjected to progressively improving flocculation conditions (all including 4 h sedimentation), in which decreasing turbidity and residual iron were observed, simultaneously with increasing microbial removal in the supernatant. Remaining Fe particles in the supernatant were typically amorphous $Fe(OH)_3$ microscopic flocs of 7−12 μm average diameter (digital microscope observations), which could be fully removed by 0.45 μm membrane filtration. The best results in terms of Fe, turbidity, and microbial removal from the supernatant were obtained for Full orthokinetic flocculation conditions. It must be noted however, that when compared to Semi-orthokinetic conditions, Full orthokinetic conditions offered just a marginal improvement in terms of Fe and turbidity removal, yet a considerable improvement in microbial removal. This demonstrates that removing approx. 0.3% additional Fe (from 0.25 to 0.11 mg/L), though apparently insignificant, adds a valuable 1.4 log_{10} removal for *E. coli* and 1.5 log_{10} removal for phage ØX174.

For all assayed configurations, *E. coli* appeared to be inactivated during the Fe-EC stage (3.9 log_{10}), after which additional inactivation was a consequence of improving floc removal, thus suggesting that the surviving bacterial cells were attached to the flocs. ROS-inactivation of phage ØX174 was poor for the first three configurations (0.8−0.9 log_{10}), rapidly increasing as flocculation acquired orthokinetic characteristics, also suggesting that incremental disinfection was a conse-

https://doi.org/10.1021/acsestwater.2c00230
ACS EST Water XXXX, XXX, XXX−XXX

quence of improving floc removal, and that the surviving viable viruses were also attached to the flocs (Figure 4).

3.3. Coupling of Mechanisms. The cumulative $\log_{10}$ removal after Fe-EC electrolysis and after sedimentation, either in the absence or presence of the ROS quencher TEMPOL is displayed in Figure 5. For these experiments, the full orthokinetic flocculation conditions were applied, with 4 h of settling time. For *E. coli*, cumulative $\log_{10}$ removal under quenched conditions is on average lower than that obtained for non-quenched conditions, although such discrepancy was statistically insignificant (ANOVA p-value $\gg$ 0.05). For phage ØX174, quenched and non-quenched data were virtually identical, with no statistical differences (ANOVA p-value $\gg$ 0.05). Figure 5 suggests that *E. coli* are likely to be partially inactivated prior or during entrapment (by Fenton intermediates) leading to a mix of viable and non-viable *E. coli* in the Fe flocs, whereas ØX174 coliphages are predominantly removed by sedimentation with a significant portion of them being still viable.

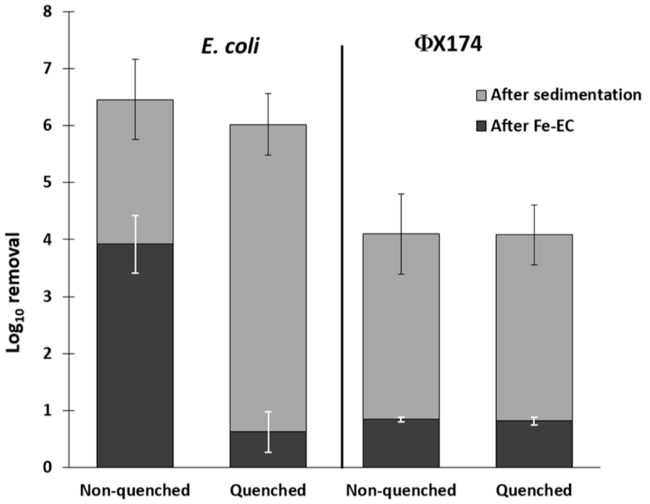

Figure 5. $\log_{10}$ removal plot of *E. coli* WR1 and phage ØX174 after Fe-EC, with and without the presence of the Fenton-inhibitor TEMPOL after Fe-EC and after 4 h settling, indicating the independent contributions of ROS inactivation and floc sedimentation. Experiments were performed in duplicate, and microbial screening was performed in triplicate. Error bars indicate standard deviation.

4. DISCUSSION

The presented results have shown that Fe floc removal was positively correlated to decreasing microbial concentrations. This indicates that both microbial indicators show affinity to be better incorporated into the floc structures and/or adsorbed onto their surface as flocculation/sedimentation conditions improve.[22,23] *E. coli* removal increased gradually from 3.9 $\log_{10}$ to >7.0 $\log_{10}$ (below detection). For phage ØX174, a sharp improvement in removal reaching 3.5 $\log_{10}$ was observed after introducing semi-orthokinetic conditions, further increasing to >5.2 $\log_{10}$ (below detection) under fully orthokinetic conditions. This type of flocculation is known to produce larger and more compact flocs with better settling ability,[33,35,36] meaning that floc sedimentation and microbial removal are faster. Under these orthokinetic conditions, it was found that *E. coli* inactivation was a result of ROS produced during Fe^{2+} oxidation, given an effective Fe-dose of approximately 50 mgFe/L. ROS inactivation appears primarily linked to the production of the hydroxyl radical ($^{\bullet}$OH) and to a lower extent to the ferryl radical (FeIV). This is concluded from the observation that under acidic conditions disinfection was orders of magnitude more efficient, which is theoretically in agreement with $^{\bullet}$OH formation.[14,39]

ROS production is a direct consequence of ferrous Fe oxidation,[14,37,38] which co-exists spatially and temporarily with the floc entrapment process. As presented in Figure 3, at a pH of 7.5 these ROS are highly detrimental to the bacterial indicator *E. coli* (3.9 $\log_{10}$), but dropped to 0.6 $\log_{10}$ when ROS were suppressed by the Fenton inhibitor. Conversely, this same ROS disinfection mechanism does not appear to affect the virus indicator ØX174 at circumneutral pH, as there is no difference in removal under quenched or non-quenched conditions, due to a reduced sensitivity of ØX174 towards the Fe(IV) radical, or to a removal process which is either ROS-independent (e.g., inactivation by Fe^{2+} or by the induced electric current) or mediated by other ROS species unable to be quenched by TEMPOL.[21] Under acidic conditions (pH 5.5) a marginal, yet statistically significant improvement in phage ØX174 inactivation was observed, evidencing a mild sensitivity to $^{\bullet}$OH radicals. However, other researchers have suggested that this could be a simple consequence of better virus sorption onto the Fe-hydroxides at lower pH, promoting aggregation and subsequent decrease in plaque counts,[39] and not necessarily the effect of more toxic radicals. Regardless, reducing pH appears to be a poor means of enhancing virus disinfection during Fe-EC, while improvement of flocculation conditions is the major determinant in virus removal, mainly by enhancing irreversible floc-adsorption and separation, as has also been reported elsewhere.[17,23,39]

Although inactivation by ROS is clearly an interesting pathway for disinfection during Fe-EC, the overall disinfection efficiency of either indicator was statistically the same for quenched and un-quenched conditions. This could cast doubt on the real advantage of using reduced Fe forms to conduct coagulation, as opposed to using more conventional Fe-based coagulants such as $FeCl_3$ for which disinfection by sorption/sedimentation has been reported.[40] However, it is imperative to consider that ROS production offers an additional disinfection barrier, particularly for *E. coli*, which could be attractive for water reclamation or drinking water treatment.[41] Municipal effluent water treatment using ferrous-based oxidation has been shown to produce sludge with lower microbial loads,[42] which is advantageous for its handling and prospective agriculture reuse applications.

5. CONCLUSIONS

It may be concluded that during Fe-EC, floc entrapment demonstrated to be an effective microbial removal process, strongly depending on flocculation conditions, being notably enhanced by proper orthokinetic conditions. Particularly, for phage ØX174, which was found to be hardly sensitive to ROS, removal patterns closely followed that of Fe removal. For *E. coli*, disinfection by ROS was found to reach 3.9 $\log_{10}$, whereas subsequent floc entrapment during sedimentation added another 3.1 $\log_{10}$. With 7.0 $\log_{10}$ *E. coli* removal, Fe-EC may be considered an effective disinfection technology. pH was found to largely influence *E. coli* inactivation by ROS, with 5.1 $\log_{10}$, 3.9 $\log_{10}$, and 1.2 $\log_{10}$ for pH 5.5, 7.5, and 8.5, respectively. This indicates that hydroxyl radicals are more

https://doi.org/10.1021/acsestwater.2c00230
ACS EST Water XXXX, XXX, XXX−XXX

effective in inactivating *E. coli* than ferryl radicals. However, the overall necessity of ROS to achieve this log removal may however be debated, as experiments where ROS was quenched by TEMPOL showed no significant difference. As such, inactivation of *E. coli* by ROS during Fe^{2+} oxidation may be considered of value for microbiologically safer sludge, as well as an additional double barrier for disinfection.

AUTHOR INFORMATION

Corresponding Author

Bruno Bicudo − *Faculty of Civil Engineering and Geosciences, Water Management Department, TU Delft, Delft, The Netherlands;* orcid.org/0000-0001-7506-0065; Email: b.bicudoperez@tudelft.nl

Authors

Bart-Jan van der Werff − *Faculty of Civil Engineering and Geosciences, Water Management Department, TU Delft, Delft, The Netherlands*

Gertjan Medema − *Faculty of Civil Engineering and Geosciences, Water Management Department, TU Delft, Delft, The Netherlands; KWR Water Research Institute, 3433 PE Nieuwegein, The Netherlands; Michigan State University, 48824 East Lansing, Michigan, United States*

Doris van Halem − *Faculty of Civil Engineering and Geosciences, Water Management Department, TU Delft, Delft, The Netherlands*

Complete contact information is available at: https://pubs.acs.org/10.1021/acsestwater.2c00230

Notes

The authors declare no competing financial interest.

ACKNOWLEDGMENTS

The authors would like to express their gratitude to NWO TTW (LOTUS-HR, grant no. 15424) for their sponsorship. We would like to acknowledge Armand Middeldorp from the TU Delft Waterlab for his constant assistance, and our intern Ruby-Jane Crichlow for her impeccable work and dedication.

ADDITIONAL NOTE

[a]Disinfection is the process of water treatment to eliminate (pathogenic) microorganisms. Elimination mechanisms are inactivation of the microorganism or physical removal of the microorganism from the water matrix.

REFERENCES

(1) Exall, K.; Vassos, T. Integrated Urban Water Management: Water Use and Reuse. *Metropolitan Sustainability*; Woodhead Publishing Series in Energy, 2012.

(2) Saidan, M. N.; Al-Addous, M.; Al-Weshah, R. A.; Obada, I.; Alkasrawi, M.; Barbana, N. Wastewater Reclamation in Major Jordanian Industries: A Viable Component of a Circular Economy. *Water* **2020**, *12*, 1276.

(3) FAO. The Wealth of Waste: The Economics of Wastewater Use in Agriculture. *FAO Water Report*, 2010; Vol. 35, pp 1−142. http://www.fao.org/docrep/012/i1629e/i1629e.pdf.

(4) WHO. 10 global health issues to track in 2021. 2021 (accessed May 1, 2022). https://www.who.int/news-room/spotlight/10-global-health-issues-to-track-in-2021.

(5) Malinovic, B.; Bjelić, D.; Đuričić, T. The phosphate removal efficiency electrocoagulation wastewater using iron and aluminum electrodes. *Bull. Chem. Technol. Bosnia Herzegovina* **2016**, *47*, 33−38.

(6) Hamdan, S. S.; El-Naas, M. H. Characterization of the removal of Chromium(VI) from groundwater by electrocoagulation. *J. Ind. Eng. Chem.* **2014**, *20*, 2775−2781.

(7) Amrose, S.; Gadgil, A.; Srinivasan, V.; Kowolik, K.; Muller, M.; Huang, J.; Kostecki, R. Arsenic removal from groundwater using iron electrocoagulation: Effect of charge dosage rate. *J. Environ. Sci. Health, Part A: Toxic/Hazard. Subst. Environ. Eng.* **2013**, *48*, 1019−1030.

(8) Lacasa, E.; Cañizares, P.; Sáez, C.; Fernández, F. J.; Rodrigo, M. A. Electrochemical phosphates removal using iron and aluminium electrodes. *Chem. Eng. J.* **2011**, *172*, 137−143.

(9) Moreno-Casillas, H. A.; Cocke, D. L.; Gomes, J. A. G.; Morkovsky, P.; Parga, J. R.; Peterson, E. Electrocoagulation mechanism for COD removal. *Sep. Purif. Technol.* **2007**, *56*, 204−211.

(10) Bazrafshan, E.; Mahvi, A. H.; Nasseri, S.; Mesdaghinia, A. R.; Vaezi, F. Removal of cadmium from industrial effluents by electrocoagulation process using iron electrodes. *Iran. J. Environ. Health Sci. Eng.* **2006**, *3*, 261−266.

(11) Jiménez, C.; Sáez, C.; Martínez, F.; Cañizares, P.; Rodrigo, M. A. Electrochemical dosing of iron and aluminum in continuous processes: A key step to explain electro-coagulation processes. *Sep. Purif. Technol.* **2012**, *98*, 102−108.

(12) Lakshmanan, D.; Clifford, D. A.; Samanta, G. Ferrous and ferric ion generation during iron electrocoagulation. *Environ. Sci. Technol.* **2009**, *43*, 3853−3859.

(13) Sasson, M. B.; Calmano, W.; Adin, A. Iron-oxidation processes in an electroflocculation (electrocoagulation) cell. *J. Hazard. Mater.* **2009**, *171*, 704−709.

(14) Hug, S. J.; Leupin, O. Iron-catalyzed oxidation of Arsenic(III) by oxygen and by hydrogen peroxide: pH-dependent formation of oxidants in the Fenton reaction. *Environ. Sci. Technol.* **2003**, *37*, 2734−2742.

(15) Galeano, L.-A.; Guerrero-Flórez, M.; Sánchez, C.-A.; Gil, A.; Vicente, M.-Á. Disinfection by Chemical Oxidation Methods. *Applications of Advanced Oxidation Processes (AOPs) in Drinking Water Treatment*; Gil, A., Galeano, L. A., Vicente, M. Á., Eds.; Springer International Publishing, 2017; pp 257−295.

(16) Dimapilis, E. A. S.; Hsu, C. S.; Mendoza, R. M. O.; Lu, M. C. Zinc oxide nanoparticles for water disinfection. *Sustainable Environ. Res* **2018**, *28*, 47−56.

(17) Kim, K.; Narayanan, J.; Sen, A.; Chellam, S. Virus Removal and Inactivation Mechanisms during Iron Electrocoagulation: Capsid and Genome Damages and Electro- Fenton Reactions. *Environ. Sci. Technol.* **2021**, *55*, 13198−13208.

(18) Villaseñor, M. J.; Ríos, Á. Nanomaterials for water cleaning and desalination, energy production, disinfection, agriculture and green chemistry. *Environ. Chem. Lett.* **2018**, *16*, 11−34.

(19) Giannakis, S. Analogies and differences among bacterial and viral disinfection by the photo-Fenton process at neutral pH: a mini review. *Environ. Sci. Pollut. Res.* **2018**, *25*, 27676−27692.

(20) Vatansever, F.; de Melo, W. C. M. A.; Avci, P.; Vecchio, D.; Sadasivam, M.; Gupta, A.; Chandran, R.; Karimi, M.; Parizotto, N. A.; Yin, R.; Tegos, G. P.; Hamblin, M. R. Antimicrobial strategies centered around reactive oxygen species - bactericidal antibiotics, photodynamic therapy, and beyond. *FEMS Microbiol. Rev.* **2013**, *37*, 955−989.

(21) Bicudo, B.; Medema, G.; van Halem, D. Van. Journal of Water Process Engineering Inactivation of Escherichia coli and somatic coliphage Φ X174 by oxidation of electrochemically produced Fe^{2+}. *J. Water Proc. Eng.* **2022**, *47*, 102683.

(22) Delaire, C.; van Genuchten, C. M.; Amrose, S. E.; Gadgil, A. J. Bacteria attenuation by iron electrocoagulation governed by interactions between bacterial phosphate groups and Fe(III) precipitates. *Water Res.* **2016**, *103*, 74−82.

(23) Heffron, J.; McDermid, B.; Maher, E.; McNamara, P. J.; Mayer, B. K. Mechanisms of virus mitigation and suitability of bacteriophages as surrogates in drinking water treatment by iron electrocoagulation. *Water Res.* **2019**, *163*, 114877.

(24) Jeong, J.; Kim, J. Y.; Yoon, J. The role of reactive oxygen species in the electrochemical inactivation of microorganisms. *Environ. Sci. Technol.* **2006**, *40*, 6117−6122.
(25) Tanneru, C. T.; Chellam, S. Mechanisms of virus control during iron electrocoagulation - Microfiltration of surface water. *Water Res.* **2012**, *46*, 2111−2120.
(26) Blount, Z. D. The natural history of Model Organisms: The unexhausted potential of E. *coli*. *eLife* **2015**, *4*, No. e05826.
(27) Payment, P.; Franco, E. Clostridium perfringens and somatic coliphages as indicators of the efficiency of drinking water treatment for viruses and protozoan cysts. *Appl. Environ. Microbiol.* **1993**, *59*, 2418.
(28) Anfruns-Estrada, E.; Bruguera-Casamada, C.; Salvadó, H.; Brillas, E.; Sirés, I.; Araujo, R. M. Inactivation of microbiota from urban wastewater by single and sequential electrocoagulation and electro-Fenton treatments. *Water Res.* **2017**, *126*, 450−459.
(29) Merzouk, B.; Gourich, B.; Sekki, A.; Madani, K.; Chibane, M. Removal turbidity and separation of heavy metals using electrocoagulation-electroflotation technique. A case study. *J. Hazard. Mater.* **2009**, *164*, 215−222.
(30) Ndjomgoue-Yossa, A. C.; Nanseu-Njiki, C. P.; Kengne, I. M.; Ngameni, E. Effect of electrode material and supporting electrolyte on the treatment of water containing Escherichia coli by electrocoagulation. *Int. J. Environ. Sci. Technol.* **2015**, *12*, 2103−2110.
(31) Hu, Y.; Wang, J.; Sun, H.; Wang, S.; Liao, X.; Wang, J.; An, T. Roles of extracellular polymeric substances in the bactericidal effect of nanoscale zero-valent iron: Trade-offs between physical disruption and oxidative damage. *Environ. Sci.: Nano* **2019**, *6*, 2061−2073.
(32) Wilcox, C. S.; Pearlman, A. Chemistry and antihypertensive effects of tempol and other nitroxides. *Pharmacol. Rev.* **2008**, *60*, 418−469.
(33) Crittenden, J. C.; Trussell, R. R.; Hand, D. W.; Howe, K. J.; Tchobanoglous, G. *MHWs Water Treatment Principles and Design*; Wiley, 2017.
(34) Eslamian, S. *Urban Water Reuse Handbook*, 1st ed.; CRC Press, 2016.Retrieved from https://www.perlego.com/book/1599053/urban-water-reuse-handbook-pdf (Original work published 2016).
(35) Wang, L.; Shammas, N.; Selke, W.; Aulenbach, D. Flotation Technology. *Flotation Technology*; Humana Press, 2010.
(36) Wiesner, M. R.; O'Melia, C. R.; Cohon, J. L. Optimal Water Treatment Plant Design. *J. Environ. Eng.* **1987**, *113*, 567.
(37) Kim, J. Y.; Lee, C.; Love, D. C.; Sedlak, D. L.; Yoon, J.; Nelson, K. L. Inactivation of MS2 coliphage by ferrous ion and zero-valent iron nanoparticles. *Environ. Sci. Technol.* **2011**, *45*, 6978−6984.
(38) van Genuchten, C. M.; Peña, J. Mn(II) Oxidation in Fenton and Fenton Type Systems: Identification of Reaction Efficiency and Reaction Products. *Environ. Sci. Technol.* **2017**, *51*, 2982−2991.
(39) Nieto-Juarez, J. I.; Kohn, T. Virus removal and inactivation by iron (hydr)oxide-mediated Fenton-like processes under sunlight and in the dark. *Photochem. Photobiol. Sci.* **2013**, *12*, 1596−1605.
(40) Payment, P.; Armon, R.; Gerba, C. P. Virus removal by drinking water treatment processes. *Crit. Rev. Environ. Control* **1989**, *19*, 15−31.
(41) Moreno, A.; Lorenzo, E.; De Bazúa, C.; De La Torre, J.; Zamora, R. M. Fenton's reagent and coagulation-flocculation as pretreatments of combined wastewater for reuse. *Water Sci. Technol.* **2003**, *47*, 145−151.
(42) Ramírez Zamora, R. M.; Orta de Velásquez, M. T.; Durán Moreno, A.; Malpica de la Torre, J. Characterisation and conditioning of Fenton sludges issued from wastewater treatment. *Water Sci. Technol.* **2002**, *46*, 43−49.
(43) American Public Health Association. *Standard Methods for the Examination of Water and Wastewater*, 23rd ed.; Baird, R., Bridgewater, L., Eds.; American Public Health Association, 2017.
(44) International Organization for Standardization. Water quality—Detection and enumeration of bacteriophages—Part 2: Enumeration of somatic coliphages. 2000, https://www.iso.org/standard/20127.html (accessed May 1, 2022).

https://doi.org/10.1021/acsestwater.2c00230
ACS EST Water XXXX, XXX, XXX−XXX